Ca Channel Kinetics during the Spontaneous Heart Beat in Embryonic Chick Ventricle Cells

Stefania Risso and Louis J. DeFelice
Department of Anatomy and Cell Biology, Emory University, Atlanta, Georgia 30322 USA

ABSTRACT The ability of Ca ions to inhibit Ca channels presents one of the most intriguing problems in membrane biophysics. Because of this negative feedback, Ca channels can regulate the current that flows through them. The kinetics of the channels depend on voltage, and, because the voltage controls the current, a strong interaction exists between voltage dependence and Ca dependence. In addition to this interaction, the proximity of pores and the local concentration of ions also determine how effectively the Ca ions influence channel kinetics. The present article proposes a model that incorporates voltage-dependent kinetics, current-dependent kinetics, and channel clustering. We have based the model on previous voltage-clamp data and on Ca and Ba action currents measured during the action potential in beating heart cells. In general we observe that great variability exists in channel kinetics from patch to patch: Ba or Ca currents have low or high amplitudes and slow or fast kinetics during essentially the same voltage regime, either applied step-protocols or spontaneous cell action potentials. To explain this variability, we have postulated that Ca channels interact through shared ions. The model we propose expands on our previous model for Ba currents. We use the same voltage-dependent rate constants for the Ca currents that we did for the Ba currents. However, we vary the current-dependent rate constants according to the species of the conducting ion. The model reproduces the main features of our data, and we use it to predict Ca channel kinetics under physiological conditions. Preliminary reports of this work have appeared (DeFelice et al., 1991, *Biophys. J.* 59:551*a*; Risso et al., 1992, *Biophys. J.* 61:248*a*).

INTRODUCTION

Diversity of Ca channels

The flow of Ca ions into excitable cells directly modulates the membrane voltage, and it acts as a messenger to regulate vesicle secretion, muscle contraction, gene expression, and a variety of other functions essential to the cell. The various roles of Ca ions depend on the spatial distribution and the temporal activity of Ca channels, i.e., where and when the Ca enters the cell, propagates through it, and initiates its action. Ca channels come in various types, and nervous tissue, skeletal muscle, smooth muscle, and the myocardium usually contain diverse categories. To explain the diversity of these excitable tissues, we usually assume that different kinds of Ca channels reside in specific locations: channel types have particular kinetics that facilitate their identification and define their function. For the most part, we equate functionally distinct channels with structurally distinct molecular entities. Indeed, evidence mounts in support of the molecular diversity of Ca channels (Mikami et al., 1989; Catterall, 1991; Mori et al., 1991; Singer et al., 1991; Tsien et al., 1991; Varadi et al., 1991; Nargeot et al., 1992; Perez-Reyes et al., 1992; Williams et al., 1992; Soong et al., 1993).

In cardiac cells, two types of Ca channels exist, the L-type and the T-type (Nilius et al., 1985; Bean, 1985, 1989; Hirano et al., 1989). Dihydropyridines modulate L channels, and isoproterenol increases their activity (Trautwein, 1984; Kokubun and Reuter, 1984; Hess et al., 1984; Nowycky et al., 1985; Hartzell, 1988; Lacerda and Brown, 1989; Josephson and Sperelakis, 1990; Yue et al., 1990; Lew et al., 1991). Dihydropyridines and isoproterenol have little effect on T channels (Tytgat et al., 1988; Hirano et al., 1989). Furthermore, L and T channels differ in their voltage-dependence: L currents have a low threshold and a slow inactivation, whereas T currents have a high threshold and a fast inactivation. Finally we note that the relative distribution of L and T channels may correlate with the development of cardiac tissues (Kawano and DeHaan, 1989; Osaka and Joyner, 1991). Thus the myocardium, as other tissues, appears to conform to general pattern of diversity of channels for disparate function.

Ca-induced inactivation

Another feature that distinguishes L and T channels is their permeability. L channels have larger conductances for Ca, Ba, or Na ions (Hess and Tsien, 1984; Nilius et al., 1985; Hess et al., 1986; Lansman et al., 1986, Levi and DeFelice, 1986; Mazzanti and DeFelice, 1987a, 1990; Yue and Marban, 1990). Ca and Ba ions themselves play a role in the inactivation of L channels, but apparently this is not true not for T channels (Hirano et al., 1989; Mazzanti et al., 1991). Thus, these two categories of Ca channel that are found in cardiac tissue seem solidly separable.

The significant property of Ca-mediated inactivation has an extended literature. Hagiwara and Najaima (1966) first showed that Ca alters the excitable of muscle fibers. Brehm and Eckert (1978), Tillotson (1979), Brehm et al. (1980), Ashcroft and Standfield (1981), and Chad and Eckert (1984) followed this suggestion with direct evidence for the involvement of internal Ca in the permeability of membranes to Ca. This work eventually led to the general concept that Ca ions,

Received for publication 14 August 1992 and in final form 1 June 1993.

0006-3495/93/09/1006/13 $2.00

as they enter the cell through Ca channels, can inactivate those same channels, and Ca-induced inactivation of Ca channels is demonstrable in a variety of cells that contain many Ca channels. The question remains whether one Ca channel can inactivate itself, or whether some form of cooperation must exist between channels for Ca-induced inactivation to occur. To discuss this issue, we have first to distinguish between voltage inactivation and Ca-induced inactivation. In cardiac cells, both kinds of inactivation would appear to exist as separate mechanisms (Hadley and Lederer, 1991). Although voltage-dependent inactivation has a well-understood role in membrane excitability, the role of Ca-inactivation remains speculative (Mentrard et al., 1984; Kass and Sanguinetti, 1984; Lee et al., 1985; Hadley and Hume, 1987; Argibay et al., 1988, Hadley and Lederer, 1991; Mazzanti et al., 1991; Yue et al., 1991; Imredy and Yue, 1992). This paper focuses on the interactions that occur between voltage inactivation and Ca-induced inactivation, and it suggests a role for this interplay under physiological conditions.

Channel-channel interactions

Heart cells conveniently demonstrate these interactions because the potential, the current, and the amount of available Ca influence one another during every beat cycle. The proximity of channels, which we refer to as channel clustering, should also play a role. For example, we would expect adjacent channels to interact more strongly than distant channels. In this case, Ca-induced inactivation would also depend on channel clustering. Even voltage-clamped membranes should demonstrate channel-channel interactions. As an illustration, discussed in more detail in DeFelice (1993), imagine a high (but uniform) channel density for which the interchannel distances were still too great for Ca-mediated interactions. Compare that situation with a low (but nonuniform) channel density in which clusters of channels exist that permit such interactions. The kinetics and therefore the functional characteristics of these two distributions would be quite different, even if the channels themselves were individually identical.

Models

This picture of channel-channel interaction raises the following possibility: functional diversity may result not only from molecular differences but also from the interactions between intrinsically similar channels. Standen and Stanfield (1982) have proposed a model in which Ca currents inactivate, because the Ca in a submembrane compartment binds to the channel. They assumed that binding either occurs instantly, or that an inactivation variable analogous to h in the Hodgkin and Huxley description (1952) depends on Ca. Thus, in the Standen and Stanfield model, Ca-induced inactivation is an intrinsic property of every Ca channel. In their macroscopic model, Ca enters a compartment via the membrane, leaves at a rate proportional to its concentration, and the current feeds back on itself uniformly. We have proposed a stochastic model of Ca channel interactions based on single-channel data (Mazzanti and DeFelice, 1990; Mazzanti et al., 1991). These data provided the initial evidence for cross-talk between Ca channels. In the earlier versions of the experiment, we used Na, Ba, or high concentrations of Ca to increase the single-channel conductance (Reuter et al., 1983; Cavalie et al., 1983, 1986; Nilius et al., 1985; McDonald et al., 1986; Klockner et al., 1990). If we used Na or Ba ions to carry the current, the channels uniformly remain open for very long times, practically throughout the entire plateau and early repolarization phase of the cardiac action potential. If we used Ca to carry the current, the Ca the channels have rather assorted kinetics: the channels generally close rapidly after voltage stimulation, although they occasionally stay open for periods that rival the regular Na or Ba opening. Thus, while Na and Ba conveniently increase the conductance of Ca channels, they significantly perturb the kinetics of the channels. A possible alternative would be to use high concentrations of Ca ions to increase conductance. However, it remains controversial whether high Ca concentration alters Ca channels kinetics. At any rate, it seems rather difficult to record from individual Ca channels without perturbing them. One of the unsolved dilemmas of these biophysical approaches to Ca channel function is to understand how they work in a normal environment from data obtained in abnormal conditions.

In this paper, we do experiments in 3 mM Ba, 4.5 mM Ba, 20 Ca, and 50 mM Ca, and, from these data, we construct a model that predicts the kinetics of Ca channels in physiological Ca. We use the patch-clamp applied to beating cells, as we have in previous studies on Na and K channels (Mazzanti and DeFelice, 1987b, 1988). The model we arrive at includes an intrinsic voltage inactivation in the channel itself, an intrinsic Ca-induced inactivation mechanism, and an extrinsic coupling that exists between the channels via Ca. Thus, our model is similar to the Standen and Standfield model. However, it differs from that model in the following respects. We presume that Ca channels are stochastic pores that open and close randomly. In our model, when a channel opens, Ca ions flow into the cell, and this Ca can inactivate that very channel. This Ca can also inactivate other channels that are close to the one that opened. Even so, some very long openings may occur by chance. The present model also describes the generally slow Ba kinetics and rapid Ca kinetics by essentially the same mechanism. Channel-channel coupling occurs by assuming a transition rate to a nonconducting (blocked) state and letting that rate increase in proportion to the Ca that flows through N open channels in a cluster. Ca ions diffuse away from the cluster without ever binding to the channels. Because the concentration of Ca changes from moment to moment, the reversal potential of the channel also changes, and we have included the two effects of inactivation and reversal potential into the same formulation.

METHODS

We prepared the cardiac ventricle cells used in this study by an enzymatic digestion of 7-day chick embryo hearts Fujii et al. (1988). After 12–24 h in tissue culture medium, we wash the cells with bath solution at room temperature. The bath contains (in millimolar): 130 Na, 1.3 K, 1.5 Ca, 0.5 Mg, 135.3 Cl, 5 dextrose, 10 4-(2-hydroxyethyl)-1-piperazineethanesulfonic acid (HEPES), pH 7.35. In these experiments, the cell-attached electrode contains various solutions, which are summarized in Table 1. We made the electrodes from borosilicate glass (Corning 7052, Novato, CA) using a programmable puller (Sachs-Flaming, PC-84, Sutter Instrument). After coating the pipettes with Sylgard (Dow Corning, Midland, MI), and after fire polishing the tips to 1–3-μm diameter, the electrodes had resistances in the range of 4–10 megohms. With these electrodes, the isolated patch has a measured area of 5–7 μm^2 (Mazzanti and DeFelice, 1987b; Wellis et al., 1990). Although a 20% size range exists from patch to patch, we attribute the variability in action currents to membrane channel density or to channel clustering, rather than to variable patch area. After forming a seal, we always examine the patch for I_{Na}, I_K, and I_{K1} channels and exclude patches that contain either these channels or any unidentified channels (Fig. 1). From previous studies, we know that these particular cardiac cells contain only dihydropyridine-sensitive Ca currents. To increase the conductance of the L-type channels underlying the dihydropyridine-sensitive currents, we use Ba or high concentration of Ca in the pipette solution (Table 1). To measure the action potential, we generally break the patch at the end of an experiment and record the first few action potentials that occur. We assume that this time-varying membrane voltage corresponds to the potential of the cell before breaking the patch. We also use blank action current traces, in which no channel openings occur, to estimate the shape of the action potential.

In previous experiments we measured leak conductance of the patch membrane by an iteration routine, in which we fit patch currents to the equation: $c(dV/dt) + gV + i_o$, where c is the patch capacitance, g is the patch conductance, and i_o is the baseline current (Wellis et al., 1990). Based on this procedure, we used the noise levels of the blank traces to estimate the leak pathway, g, approximately 250 gigohms in the data reported here. The cells have a diameter of 10–13 μm, and they have resistances between 1 and 10 gigohms. For this report, we used single cells exclusively.

We used a List EPC-7 to measure the current. We bandlimit the data at 1000 Hz and applied a subtraction routine to all traces (omitting Figs. 1 and 2, which illustrate the raw data). In cell-attached patch experiments, with the bath potential set at 0 mV, the cell action potential appears across the patch membrane. Adding positive 20 mV to the pipette shifts the action potential negative by 20 mV, etc. In this way, we are able to shift the voltage across the patch to test our theory against the data. We store the data on a VCR and use a Nicolet 4094 oscilloscope and IBM-AT computer to analyze them. The modeling procedures make use of MCHAN, a program written by Bill Goolsby and Lou DeFelice (DeFelice et al., 1989) for IBM-compatible machines running DOS 3.0 (or later) with 640K RAM, a math coprocessor, and Hercules CGA, VGA, EGA, or compatible color graphics. MCHAN outputs an ASCII format that can transfer to other programs for further processing. We will provide copies of this program on request.

RESULTS

All of the data presented in this paper come from cell-attached patch experiments on individual cells isolated in primary tissue cultures from 7-day chick ventricle. We use a physiological solution in the bath to sustain cell beating. The pipette solution (see Methods) is designed to discriminate against all channels other than Ca channels. However, we often see K channels in the patch, or unidentified channels, and we simply reject these. To enhance the current through Ca channels, we use a variable concentration of Ba or Ca (Table 1). Fig. 1 shows consecutive action currents (*rows*) from different patches (*columns*) recorded from spontaneously active cells. The pipette solution in this case contains 3 mM Ba, and we have not subtracted the capacitive transient. The action potentials remained virtually identical from beat to beat throughout a given experiment; nevertheless, action currents appear to have rather different kinetics. The top row shows action currents from patches that contain both inward and outward currents. This exemplifies an experiment that we would reject. We accept patches for analysis that contain only downward currents, like those shown in the bottom three rows, which we assign as Ca channel openings by elimination. The traces illustrated in Fig. 1 attempt to show the range of action currents that we see in our experiments, viz., 1) brief openings that occur somewhat randomly throughout the action potential; 2) relatively short-lived currents that occur just after the upstroke; and 3) bursts of openings that last for hundreds of milliseconds. The theory of Ca

TABLE 1 Solutions

			Pipette			
	Bath	Internal	3.0 Ba	4.5 Ba	20 Ca	50 Ca
			mM			
NaCl	130.0	0	124	121	88	28
$CaCl_2$	1.5	0.1	0	0	20	50
$BaCl_2$	0	0	3	4.5	0	0
$MgCl_2$	0	2	0.5	0.5	0.5	0.5
$MgSO_4$	0.5	0	0	0	0	0
KH_2PO_4	1.3	0	0	0	0	0
KCl	0	120	1.3	1.3	1.3	1.3
HEPES	10	10	10	10	10	10
EGTA	0	1.1	0	0	0	0
Dextrose	34	30	5	5	10	40
pH	7.35	7.35	7.35	7.35	7.35	7.35
Osm (mOsm)	300	270	280	280	270	270
4-AP	0	0	10	10	10	10
TEA	0	0	5	5	5	5
TTX	0	0	0.001	0.001	0.001	0.001

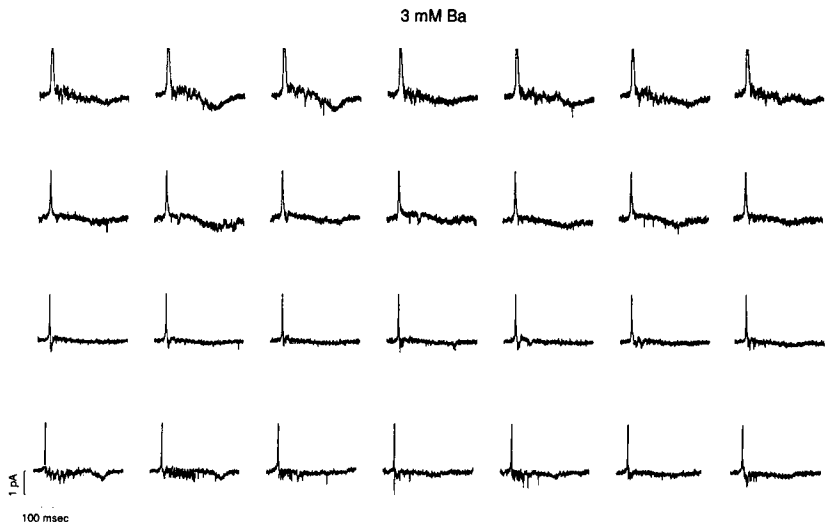

FIGURE 1 3 mM Ba: sample action currents before capacitive and leak subtraction. Sequential action currents from four different patches on spontaneously beating, 7-day chick ventricle cells at room temperature. The bath contains a physiological solution, and the pipette contains a 3 mM Ba solution (see Methods). These action currents represent the range that we see in our experiments: the top row illustrates a patch that we discard, because the currents are upward, and downward in spite of our attempt to select for Ca channels with the pipette solution; the bottom three rows show patches we would retain for analysis. They illustrate the wide variability in channel openings, not only from patch to patch, but also from beat to beat.

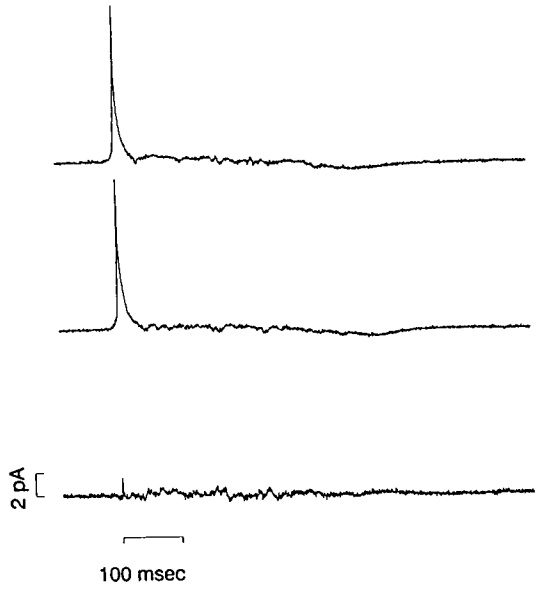

FIGURE 2 Method of consecutive-beat subtraction. Illustration of the consecutive-beat subtraction method use in the remainder of the paper. Top traces: two sequential action currents from a cell-attached patch on a spontaneously beating 7-day chick ventricle cell at room temperature. Bottom trace: the difference current. The bath contains a physiological solution; the pipette contains a 3 mM Ba solution. The fast upstroke of the action potential causes the sharp outward current, seen near the beginning of each of the top two traces in Fig. 2. This current, which is largely a capacitive current from the patch, allows us to line up the two traces for subtraction. (The slow inward current, seen toward the end of each of the top two traces, represents the repolarization of the action potential.) By merely subtracting each action current from the previous one, we eliminate background currents but retain the randomly opening, and closing ionic currents. Using consecutive beats insures that we subtract virtually identical capacitive and leak currents. This procedure causes the ionic currents, which are downward as raw data (Fig. 1), to become downward and upward deflections.

channel kinetics that we present here accounts for these different kinetics and offers an explanation for the underlying cause of this incongruous behavior.

Consecutive-beat subtraction method

We have found it convenient in these experiments to eliminate background currents by subtracting consecutive action currents. This method assumes that capacitive and leak currents remain constant over adjacent beats, and it assumes that channel openings occur randomly. The difference trace that results from the subtraction of course inverts one set of channel currents; nevertheless, the difference trace shows the temporal activity of the channels and the amplitude of the current rather well (Fig. 2), and the data can easily be compared with the theory if we perform the same manipulation on the simulated data. All of the subsequent experiments after Fig. 3 use the method of consecutive-beat subtraction, and in Fig. 7 we use the same representation to compare the data with a model.

Fig. 3 contrasts two cells under nearly identical conditions. Both patch pipettes contain the 50 mM Ca solution, and the action potentials have very nearly the same shape and duration. In spite of these similarities, the action currents have rather different kinetics. When the pipette voltage equals 0 mV, the patch membrane experiences the same action potential as the cell. In the experiment illustrated on the left, the channels open early and they remain active quite late in the action potential. Hyperpolarization of the patch action potential causes the channels to close earlier and the open times to become shorter. For the experiment on the right, the action currents have a larger amplitude initially. These channels also close earlier, and their kinetics do not change much when we hyperpolarize the patch. Fig. 4 repeats the protocol of Fig. 3, but with the 20 mM Ca solution in the pipettes. For the experiment on the left, small currents last throughout the action potential when the offset potential is set to 0 mV. Hyperpolarization of the patch promotes the occurrence of late openings with large amplitudes, and some channels even open before the action potential upstroke. For the experiment on the right, the currents are generally smaller than on the left, and they are hardly measurable unless we hyperpolarize

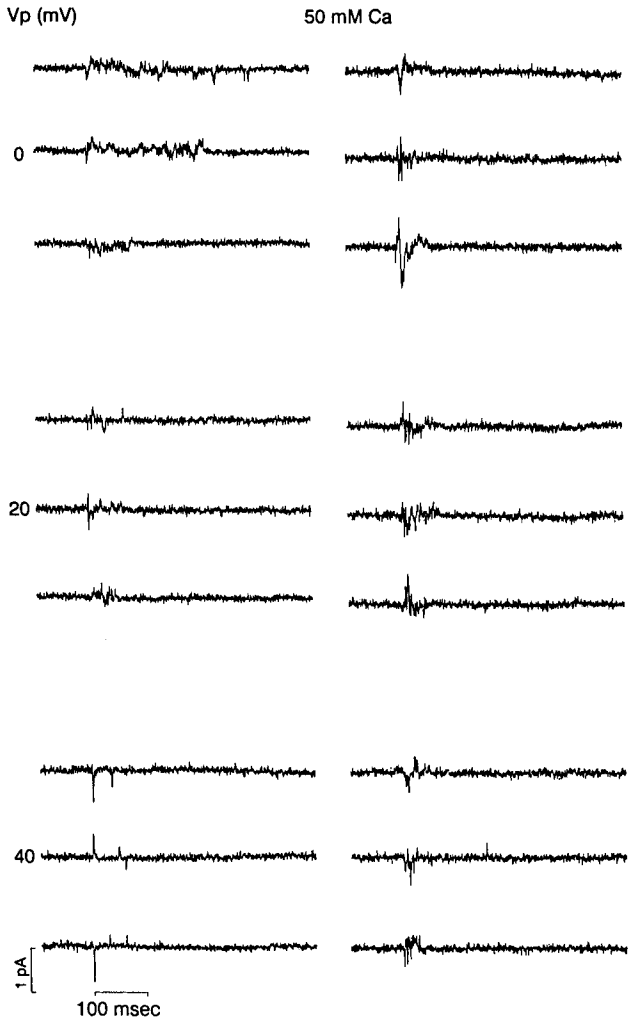

FIGURE 3 50 mM Ca: consecutive-beat subtraction. Selected action currents from cell-attached patches on two different spontaneously beating 7-day chick ventricle cells at room temperature. The bath contains a physiological solution. The pipette contains 50 mM Ca. Each trace results from the procedure illustrated in Fig. 2. The pipette potential, V_p, hyperpolarizes the action potential in the patch without disturbing the rest of the cell. Left column: in this cell, the activity change with V_p: at 0 mV; openings persist into the late plateau, and early repolarization phase; at 20- and 40-mV hyperpolarization the openings become more brief and occur mainly during the early plateau phase. Right column: in another cell under the same conditions, the kinetics show a different pattern; at 0 mV the initial current stands out clearly, but channels close sooner; hyperpolarization has little effect. The left edge of the 100-ms time scale indicates the upstroke of the action potential.

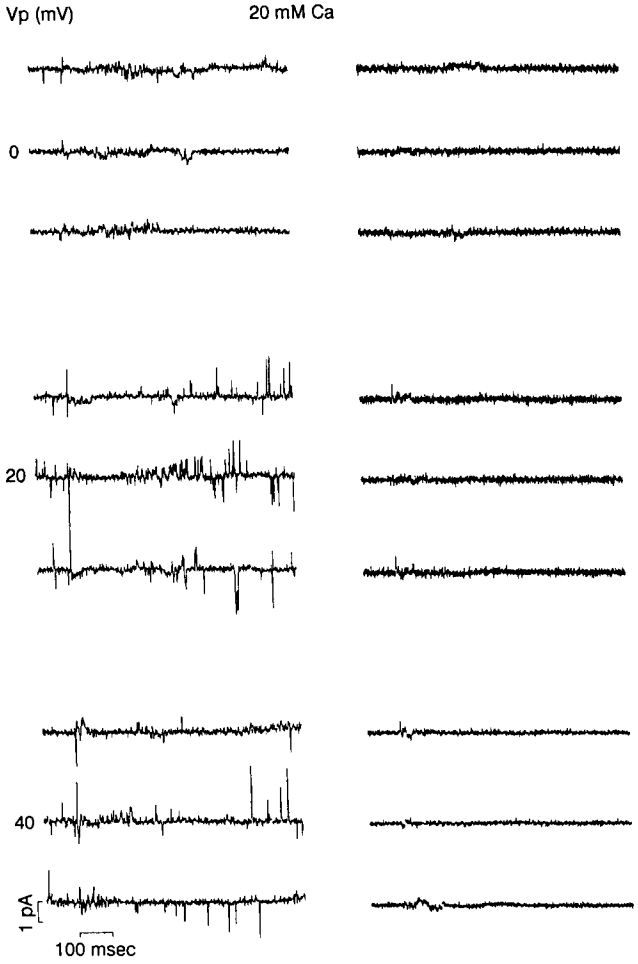

FIGURE 4 20 mM Ca: consecutive-beat subtraction. This experiment repeats Fig. 3, but with 20 mM Ca in the pipettes. Left column: in this cell, the activity of the Ca channels change as V_p changes; at 0 mV openings occur through action potential into the late plateau and early repolarization phase; at 20- and 40-mV hyperpolarization the openings continue throughout the action potential, but they become briefer during the late phase. Right column: another cell shows a different pattern; at 0 mV no initial current appears; hyperpolarization has a small effect on amplitude.

the patch by 20 or 40 mV. Fig. 5 again repeats the protocol of Fig. 3, but now with two electrodes on the same cell rather than two different cells. This experiment essentially guarantees that the action potentials are identical for the two patches, something we have no assurance of in two different cells. Though the action potentials are the same, two different kinds of action currents occur in the separated patches. For the patch represented on the left, rather small action currents last throughout the action potential; for the patch on the right, the initial currents are larger and their amplitude falls off noticeably during the late action potential. For each of these patches, we show sample action currents as well as the average current from 60 sequential traces. Although the individual traces show great variability, the average traces seem only slightly different. However, the average current from the patch on the right decays faster from a larger initial value. In the remaining data figures, we have selected individual traces from characteristic experiments to illustrate this variability. Fig. 6 is an experiment with 4.5 mM Ba in the pipette. In the patch represented on the left, the channels open early and have only small currents that remain active throughout the action potential. On the right, we illustrate another extreme in which large action currents appear late in the action potential. These late currents increase in amplitude and close more rapidly if we hyperpolarize the patch action potential.

Thus, we have presented a very incongruous set of data that would seem to defy any attempt to describe them with a uniform theory. The following model attempts to apply a voltage-dependent and Ca-dependent stochastic representation of Ca channels to explain these diverse experiments. We

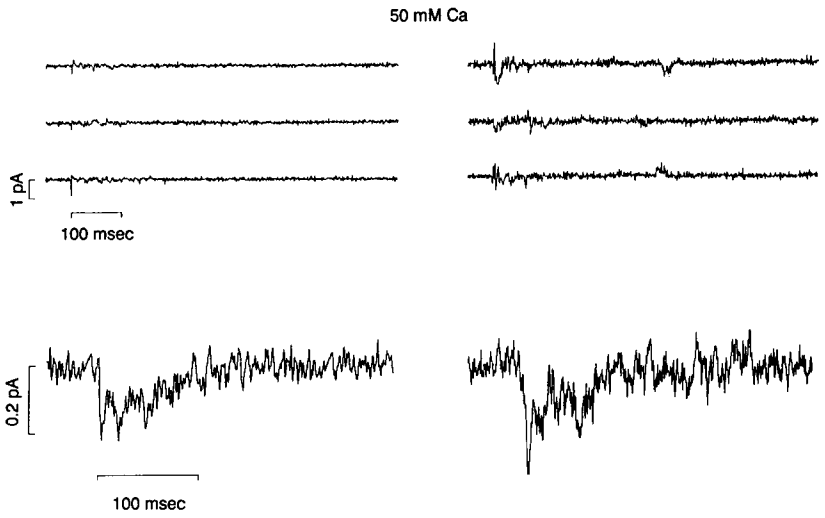

FIGURE 5 50 mM Ca: consecutive-beat subtraction; two electrodes. In this experiment, we have two pipettes on the same cell. Otherwise the conditions exactly repeat those in Fig. 3. In the patch on the left, the initial current remains throughout the action potential. On the right, the initial current declines within the first 100 ms. Below each set of examples, we show the average current from 60 sequential action currents.

begin with a state diagram based on our previous voltage-clamp data for Ba currents (see Fig. 9 in this paper, from Mazzanti et al. 1991). We have, in the present model, retained the purely voltage-dependent rate constants, α_o, β_o, α_c, β_c, α_i, β_i, α_f, β_f, that we derived for Ca channels conducting Ba. However, we have let the current-dependent rates, α_b and β_b, change according to whether we use Ba as the charge carrier, or Ca (Table 2). In either case, the current through the channels causes charge to collect according to the equation:

$$Q(t) = \exp(-t/\theta) \int_0^t \exp(u/\theta) I(u)\, du,$$

where θ is the time constant of integration, and u is a dummy variable of integration. If $I(t)$ remains constant over the computation step Δt, and if Δt is small compared to θ, then the initial charge is:

$$Q_0 \sim I_0 \Delta t_0,$$

and the subsequent charge is:

$$Q_1 \sim Q_0 + I_1 \Delta t_1 - Q_0 \Delta t_0 / \theta.$$

We use this iteration to update the rate constant β_b every Δt as follows.

$$\beta_b = kQ(t)$$

I is in μA, t is in ms, and Q is in ncoul; k is a constant that converts ncoul to ms^{-1}. The constant α_b describes the unblocking rate $B \rightarrow O$. It is a constant. All voltage-dependent rate constants obey the equation:

$$\text{Rate} = \xi \exp^{a(V-b)}/[1 + e^{a(V-b)}].$$

Table 2 lists the values that we have used for ξ, a, and b, the voltage-dependent rate constants, and θ and k, the current-dependent parameters. For the open-channel current, we use the equations

$$i(V) = \gamma(V - E)$$

$$\gamma = 10 \text{ pS in 50 mM } Ca^{2+} \text{ or 5 pS in 1.5 mM } Ca^{2+}.$$

For the reversal potential, we let

$$E = -kT/2e \ln[Ca_i/Ca_o],$$

$$Ca_i(t) = 1\ \mu M + 0.5\ \mu M \text{ fcoul}^{-1}\, Q(t)$$

$$Ca_o = 50 \text{ mM } Ca^{2+} \quad \text{or} \quad 1.5 \text{ mM } Ca^{2+}.$$

Yue and Marban (1990) and Mazzanti and DeFelice (1990) have shown that cardiac L channels have a conductance of 8–10 pS in 10 mM Ca. Yue and Marban (1990) and Imredy and Yue (1992) show that very high Ca (160 mM) elevates the conductance only slightly to 10–13 pS. Complete data on single Ca channel conductance in normal Ca concentrations do not exist (see, however, Klockner and Isenberg (1991), who report 8 pS for long openings in 2 mM Ca at 36°C). Therefore, we have extrapolated the value of 5 pS used above from Yue and Marban (1990; their Fig. 5). We used the nominal values of γ = 5 pS in 1.5 mM Ca and 10 pS in 50 mM Ca in our calculations. We used in the simulations the nominal value of 10 pS for L-type Ca channels in 4.5 mM Ba (Fig. 7). The value of 10 pS for 4.5 mM Ba agrees with the single-channel conductances we have obtained in our cells. We let external Ca remain constant and equal to the Ca concentration in the bath solution, but we allow internal Ca to vary with the total current (I). I is the current that passes through N channels which are theoretically at the same spot in the membrane and experience exactly the same voltage. Thus, the number N determines both the rate to the blocked state for each channel at that place, as well as the dynamic reversal potential for each channel at that same place. This group of channels we refer to as a cluster.

In Fig. 7, we use the model to plot the expected currents from four patches: two of the simulations correspond to the experimental protocol in Fig. 3 (50 mM Ca), and two of the simulations correspond to the experimental protocol in Fig. 6 (4.5 mM Ba). We have subtracted adjacent simulated traces (which are, of course, different by the nature of the model). This procedure duplicates the consecutive-beat subtraction method and provides us with direct visual comparison with the data. The theoretical patches contain either one or five

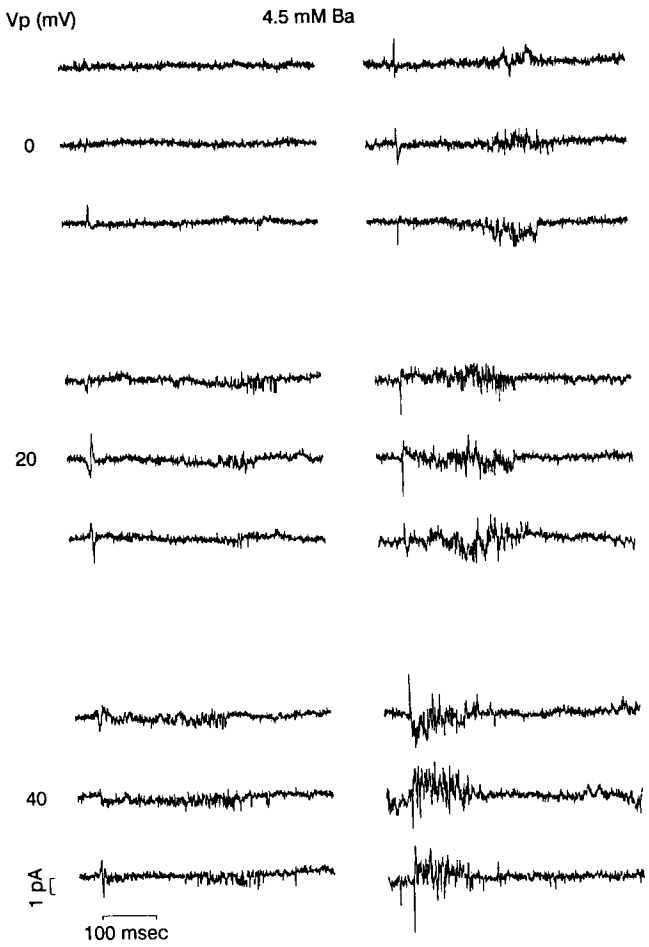

FIGURE 6 4.5 mM Ba: consecutive-beat subtraction. The experimental conditions repeat Fig. 3, but with 4.5 mM Ba in the pipettes. Left column: in this cell, the channels remain active throughout the action potential at all pipette potentials; hyperpolarization increases the current amplitude. Right column: currents are generally larger than on the left; at 0 mV activity seems greatest during the late phases of the action potential; as we hyperpolarize, amplitude increases, activity shifts to the left, and channels close sooner.

channels, and we hyperpolarize the patch action potentials by 0, 20, or 40 mV to correspond to the experiments. Compare the left column of Fig. 3 with the upper left quadrant of Fig. 7. For 50 mM Ca in the patch pipette and one channel in the patch, the model predicts that the Ca channel will open and close more or less continually throughout the action potential. This pattern occurs because the Ca currents through the single channel are generally too small to inactivate the channel (i.e., too small to shift the channel to the blocked state, B, although this may occasionally happen). As we hyperpolarize the patch, the rate to the voltage-inactivated state becomes larger and the channels close sooner for that reason. For the same 50 mM Ca condition, but now with five channels in the patch, the Ca current of course increases. However, the Ca-induced block is now much stronger, and hyperpolarization has relatively less effect on channel kinetics dominated by the blocked state. This general behavior approximates the experimental situation shown in Fig. 3. With 4.5 mM Ba in the simulated condition, and with one channel

TABLE 2 Model parameters: all rates (except β_b) = $\xi e^{a(V-b)}/[1 + e^{a(V-b)}]$ $\beta_b = k \exp(-t/\theta)\, 0^t \exp(u/\theta)I(u)du$

	a(mV)$^{-1}$	b(mV)	ξ(ms)$^{-1}$
Voltage-dependent states (CIOF)			
Ba or Ca			
α_0	0.20	−15	0.2
β_0	−0.05	−40	2.0
α_i	−0.05	−60	0.005
β_i	0.20	−50	0.005
$\alpha_f = \beta_f$	−0.10	−10	1.0
Current-dependent state (B)			
Ba			
α_b	−0.06	−80	1.0
β_b	k = 1 (ncoul ms)$^{-1}$	θ = 1 s	
Ca			
α_b	0.0	0.0	0.001
β_b	k = 0.01 (ncoul ms)$^{-1}$	θ = 100 ms	

in the patch, the model predicts a small Ba current during the action potential. If we hyperpolarize the patch, the Ba currents become larger. The rate to Ba block is much slower than the rate to Ca block, and the Ba currents occur throughout the action potential. Notice, however, that with five channels in the patch, the Ba currents become more and more evident as the action potential repolarizes. Hyperpolarization of the patch action potential causes a shift of the Ba currents toward early openings. These kinetics approximate the data that we show in a corresponding experiment in Fig. 6.

To summarize these results, Fig. 8 shows a measured action potential and theoretical action currents for two Ca concentrations and two sets of Ca channels. In 50 mM Ca, 40 channels develop a large initial current that is followed by strong inactivation. The simulation shows that late openings of rather short-duration occur, and that these late currents give rise to a second phase of the Ca current, which is characteristic of cardiac cells during the action potential.

In 1.5 mM Ca, the current is, of course, generally smaller. With 40 channels in a cluster in 1.5 mM Ca, the total current shows a sharp, initial peak followed by a late phase, but the peak is relatively smaller than it is in 50 mM Ca. With only two channels in the cluster, the Ca current tends to have a more uniform activity throughout the action potential. The openings that occur during the plateau phase are generally longer than those that occur during repolarization. On average, therefore, the currents from two channels in 1.5 mM Ca are also biphasic. Fig. 9 plots the theoretical Ca current in 1.5 mM Ca from clusters of channels containing two or 40 pores. The kinetics of the current from either two or 40 channels show two phases, a sharp initial current followed by a slow late current. With 40 channels, the initial current is more pronounced than the repolarization current. To show this better, we normalized the two currents and plotted them together on the same time scale as the action potential (the *dotted* and *solid traces* in the bottom panel of Fig. 9). The absolute values for the peaks of these two currents are approximately 0.25 and 3.5 pA. The middle panels in Fig. 9 show the occupancy of the open state, the inactivated state, and blocked state of an average channel in a two-channel

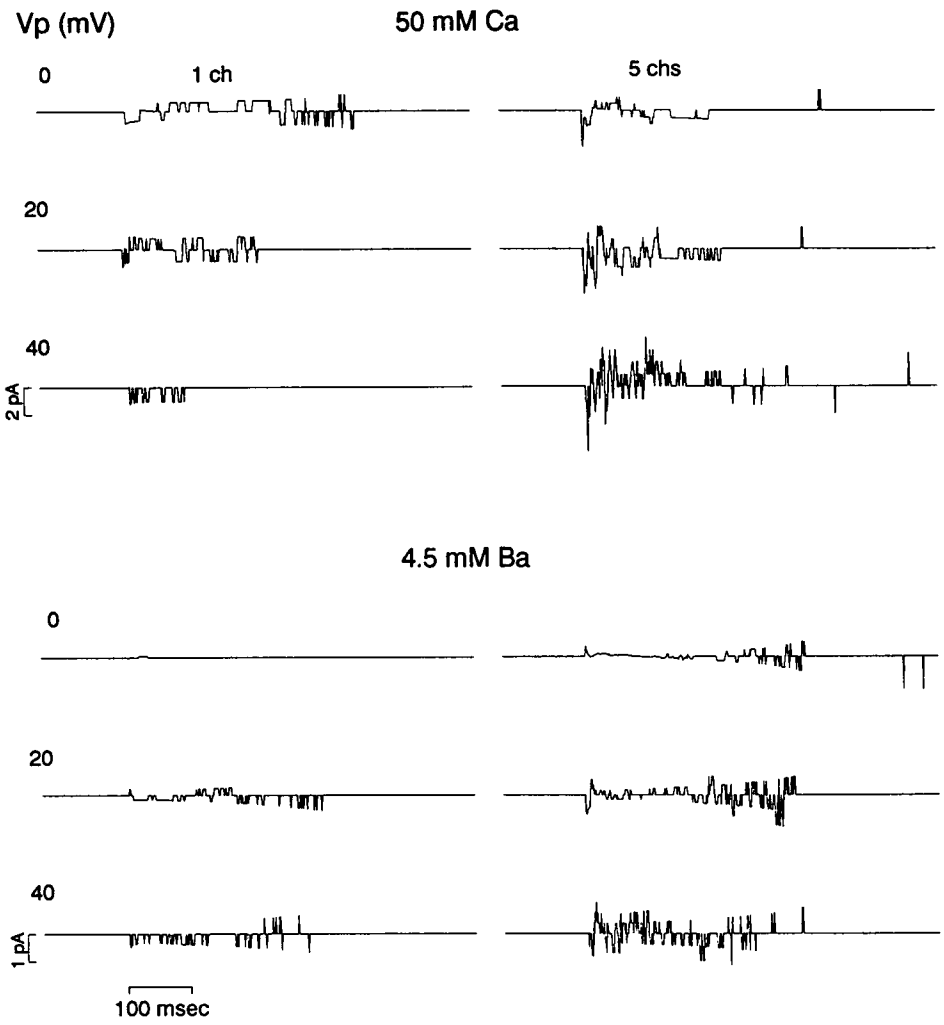

FIGURE 7 Model: trial runs. A theoretical summary of the experimental protocols used in Figs. 3 and 6. We use time increments of Dt = 0.3 ms for all calculations. The top panels simulate 50 mM external Ca in the pipette, and either one or five channels in the patch. We offset the patch action potential by 0-, 20-, or 40-mV hyperpolarization, as indicated. The action potential is shown in Fig. 8. The bottom two panels repeat the simulation with 4.5 mM Ba in the pipette. The single-channel conductance of L-type Ca channels in 50 mM Ca or 4.5 mM Ba have the same nominal value of 10 pS (see text). Each trace in Fig. 7 represents the subtraction of two consecutive computer runs.

cluster, and a 40-channel cluster, during the action potential. For either case, typically half of the channels in the cluster open during the initial depolarization. In the two-channel case, voltage inactivation dominates during the repolarization phase, and Ca inactivation plays a relatively minor role. However, in the 40-channel case, voltage and Ca inactivation play approximately equal roles. In this model, therefore, both the incomplete voltage inactivation and the incomplete Ca inactivation may contribute to the late, repolarization current. The relative contribution of these two mechanisms depends on the number of channels that interact in a cluster.

DISCUSSION

In our analysis, we have assumed that the Ca channel population consists of L-type currents, because 20 μM nifedipine abolishes all of the whole-cell Ca current or the whole-cell Ba current, and 30 μM cAMP in the patch pipette enhances these currents 2–3-fold (Mazzanti et al., 1991). By this definition, T-type channels do not exist in the 7-day chick ventricle cells that we have used in these experiments. Therefore, our model consists of a population of intrinsically identical channels. The rate constants that we have used here for the Ca channels differ from our previous model for Ba currents, but only in the extrinsic variables that depend on current. Thus, the intrinsic voltage dependence of the Ca-conducting Ca channel and the Ba-conducting Ca channel remains the same. The single-channel conductances also differ in Ba or Ca, and we have included this effect. Finally, we have allowed the Ca reversal potential to vary with the current following the same formulation as the Ca-induced inactivation. These changes in our previous model have produced a unified description for both Ba and Ca currents during either voltage-clamp experiments or spontaneous action potentials experiments.

Another method to study Ca currents during action potentials requires clamping the cell with a voltage that mimics the shape of the action potential. This method involves blocking all the currents in the cell except the Ca currents (Doerr et al., 1989, 1990; Arreola et al., 1991). The procedure, therefore, precludes any interactions that may occur between Ca channels and other channels, and it assigns all the effects to one primary cause, viz., voltage. Furthermore, the whole-cell recording electrode in such experiments perfuses the cell, which changes the ion concentrations and the metabolites near the membrane. Such differences could alter channel

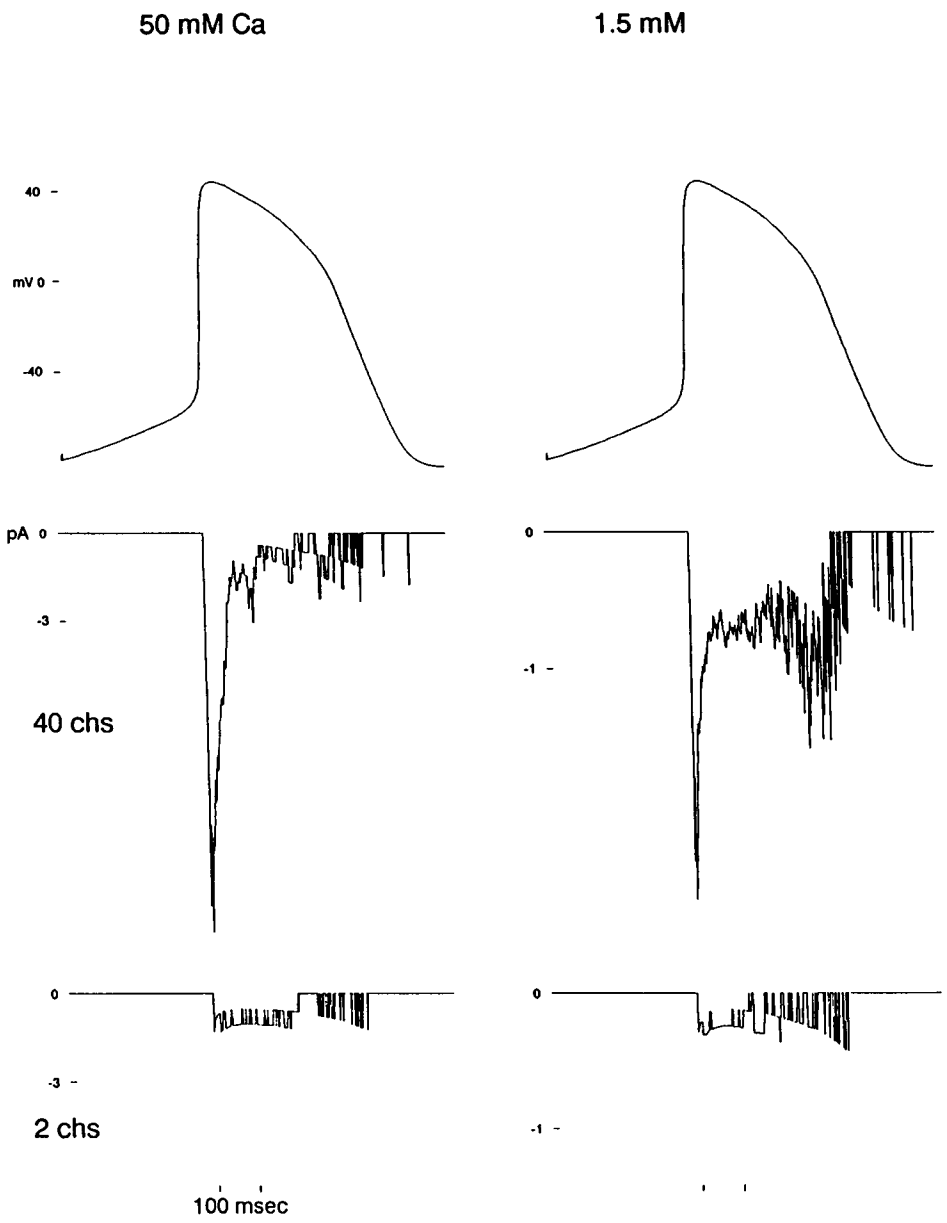

FIGURE 8 Model: trial runs. A simulation of Ca channel activity during the action potential. The measured voltage which drives the model appears at the top of each column. It is the same action potential that we used in Fig. 7. The simulated currents for 40 channels or two Ca channels lie below these action potentials. In the left column, we do the calculations with 50 mM external Ca. In the right column, we do the same calculations using 1.5 mM Ca. Note the difference in scales between the two action currents.

activity (Hartzell, 1988; Ochi and Kawashima, 1990; Armstrong et al., 1991; Hartzell et al., 1991). We generally think that studying the kinetics of channels in a cell-attached patches, without using a whole-cell electrode, introduces less perturbation. Applying the method to Ca channels, however, has presented us with some unique obstacles.

The first problem comes because the measurement of single-channel events in Ca channels usually requires ions that are more penetrating than Ca itself. Thus, researchers generally use Na or Ba ions to replace Ca in single-channel experiments. Another solution to the problem is to use high concentrations of external Ca. This seems unwarranted, however, because Yue and Marban (1990) and Mazzanti and DeFelice (1990) have shown that cardiac L channels have the reasonably high conductance (8–10 pS) in 10 mM Ca. (Klockner and Isenberg 1991, in a preliminary report, give a value of 8 pS in 2 mM Ca at 36°C, but we have cannot reproduce these data in our preparation.) Indeed, a very high concentrations of external Ca (160 mM) elevates the channel conductance by only 25% (Imredy and Yue, 1992). Thus, the idea that experiments on individual L-type Ca channels automatically requires Ba or high concentrations of Ca, would seem to warrant re-examination. Nevertheless, we have used Ba and high Ca in our present experiments. Part of the reason is to be able to compare our experiments with previous work. However, we generally cannot observe single-channel events during action potentials with normal concentration of Ca in our pipette (1.5 mM). During the action potential, the main activity of the channels occurs during the plateau phase and, therefore, near the reversal potential of the channels. Thus, during action potentials, Ca channels simply do not conduct much current: they are essentially off when the driving force is large and on when the driving force is small. Occasionally, however, they do open from states with low probability, and

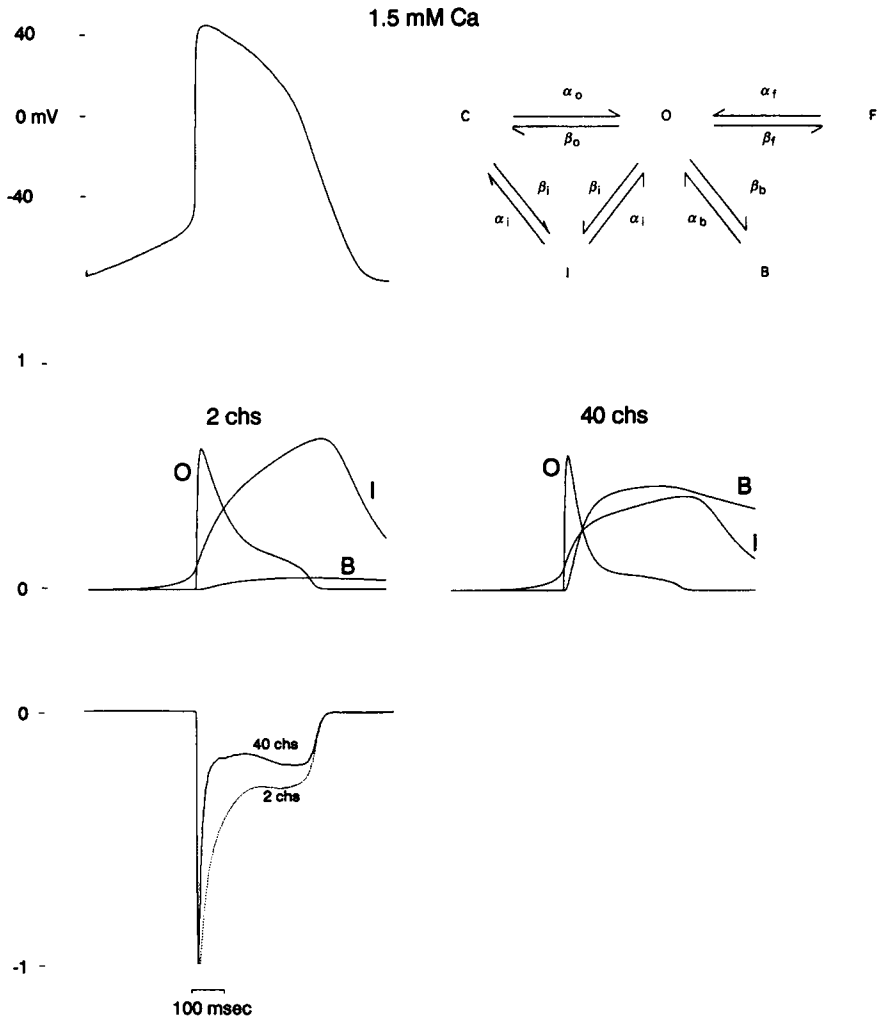

FIGURE 9 Model: average currents. Average theoretical Ca action currents for 1.5 mM Ca with two or 40 channels in a cluster. The inset shows the model we use in the present study, as originally proposed by Mazzanti et al. (1991). As in all the calculations, Table 2 gives the rate constants. The relevant equations appear in the text. The middle panels show the occupancy of states O, I, and B on the same time scale as the action potential. The bottom panel compares the two-channel current with the 40-channel current on a normalized scale. The absolute values for the peaks of these currents are approximately 0.25 and 3.5 pA.

we include this possibility in our model. We easily detect Ca channel activity with 3 mM Ba in the pipette, or with Ca in the pipette above 10 mM and extrapolated these results to predict behavior in normal Ca. For this extrapolation, we assume that our previously measured voltage-dependent rate constants apply to Ba-conducting or Ca-conducting channels at any concentration of the transported ion. Such a model suggests that voltage-dependent inactivation operates through a mechanism that is separate from current-dependent inactivation. Separation of the two mechanisms has reasonable experimental support (Kass and Sanguinetti, 1984; Bean, 1985; McDonald et al., 1986; Hadley and Hume, 1987; Hirano et al., 1989; Hadley and Lederer, 1991). In our model, we have let the rate to the Ca-blocked state occur at 100 times the intrinsic rate of Ba to the analogous state (k in Table 2). For Ca, we also let the recovery from block occur 1000 times slower (α_b), and the concentration decay occur 10 times faster (θ in Table 2) than for Ba. These nominal changes result in strong, Ca-induced inactivation compared to the smaller, but nevertheless detectable, Ba-induced inactivation. In addition, we let the Ca reversal potential depend on the Ca gradient across the channel by keeping external Ca constant and letting internal Ca vary with the total current through a cluster. The Ca that controls inactivation, and the Ca determines the reversal potential, are thus handled by exactly same formulation. The model we have developed gives a range of Ca channel kinetics that agrees with our experiments, whether we use Ba or Ca as the conducting ion (Fig. 7). Using this approach, we can predict the kinetics of Ca channels under other conditions, including physiological conditions for which it is difficult to obtain data (Fig. 9).

A second problem arises for Ca channels because the usual assumption of channel independence does not apply to Ca channels, at lease not under all circumstances. To illustrate what we mean here by independence, consider the experiments of Sigworth and Neher (1980), who showed that, for Na channels, the average kinetics of individual Na channel currents, $i(t)$, do approximate the macroscopic Na channel current, $I(t)$. This idea is usually summarized by the identity, $I = Nip$. This equation generally assumes that the same i and the same p hold for each one of the N independent channels. The relationship (viewed as representing N independent events) holds for a number of different kinds of ion channels, and one might have expected it to hold for Ca channels. Ca channels, however, do not sum independently. The identity $I = Nip$ still applies, of course, but now contingent rela-

tionships exist between i, p, and I. In voltage-clamp experiments, we have shown that one or two channels in a patch have slowly inactivating currents that are typical of L-type currents; however, eight or more channels in a patch have more rapidly inactivating currents (Mazzanti et al. (1991); 20 mM Ba). (Klockner and Isenberg (1991) mention similar effects in 2 mM Ca at 36°C.) We have modeled this cooperativity by the simple assumption that the blocking rate for *each* channel depends on the total current through N channels. Thus, Ca-mediated inactivation increases with the number of channels in a cluster.

Our present experiments and attempt to model the physiological condition of Ca channels in beating heart cells conducting Ca. These experiments indicate that great variability exists in Ca channel activity. We have suggested that this variability comes about because cardiac cells have an uneven distribution of Ca channels, which we sample by our technique more or less indiscriminately. Although we have no direct evidence for Ca channel clustering in the heart, we have nevertheless made channel clustering and channel-channel interactions a central feature of the model. In our view, individual Ca channels sufficiently isolated from other Ca channels would show very little Ca-induced inactivation, and that such inactivation is a consequence of channel clustering. We believe that the conditions under which previous experiments were done may have caused the conflicting results reported in the literature (no Ca-mediated single-channel inactivation in 40 mM Ca (Lux and Brown, 1984); Ca-mediated single-channel inactivation in 160 mM Ca (Yue et al., 1990)). In any case, more recent data supports the idea that interactions can exist between Ca channels (Imredy and Yue, 1992), and they may provide additional evidence for the presence of the submembrane spaces proposed for Na/Ca exchange currents (Lederer et al., 1990).

We propose that inactivation depends on the local clustering of Ca channels and on the buildup and removal of Ca from submembrane spaces. In cardiac cells, internal Ca may elevate from baseline values of 0.05 μM to peak values of 16 μM (Cannell et al., 1987; Arreola et al., 1991; Cleemann and Morad, 1991). In nerve, the internal Ca in submembraneous domains may be as high as 300–1000 μM (Roberts et al., 1990; Llinas et al., 1992). We selected 1 μM as the baseline concentration of Ca near the membrane of beating cells. The submembraneous concentration in spontaneously active cells will exceed the global concentration, but estimates for values adjacent to the plasma membrane do not exist for heart. In our model, Ca increases by 0.5 μM for every fcoul of integrated Ca current through the plasma membrane; at the same time Ca is building up, we let it decay with a time constant of 100 ms. We chose 0.5 μM/fcoul, because it gave peak values of 30–150 μM during an action potential. These nominal values are higher than the available estimates in heart and lower than the same estimates in nerve. Although a variety of processes must contribute to Ca dynamics under the membrane, we have lumped them together in a first order process with one decay constant, θ, and one current source, I. A more complete model might include cytosol buffering, electrostatic repulsion, diffusion, and reabsorption into the sarcoplasmic reticulum as separate decay mechanisms, and the sarcoplasmic reticulum as an additional source of current. At present, however, we do not have enough information to include these processes as independent terms in our expression for $Q(t)$.

It follows that wide diversity may result from intrinsically similar channels. Experimental conditions such as Ba or high Ca influence channel kinetics. But physiological conditions, too, such as Ca channel clustering and ion chelation, also play important roles. This view would imply that large, transient currents as well as small, long-lasting currents can arise from the same kind of channel, and it could help explain the wide dissimilarities in kinetics reported among the channels categorized as L-type.

We thank B. J. Duke for preparing the solutions and the primary cultures and W. N. Goolsby for maintaining the electronic and computer facilities. We also thank Michele Mazzanti for help with some initial experiments done on this project and for many useful discussions on the final work.
This research was supported by National Institutes of Health grant HL-27388.

REFERENCES

Argibay, J. A., R. Fischmeister, and H. C. Hartzell. 1988. Inactivation, reactivation and pacing dependence of Ca current in frog cardiocytes: correlation with current density. *J. Physiol. (Lond.).* 401:201–226.

Armstrong, D. L., M. F. Rossier, A. D. Shcherbatko, R. E. White. 1991. Enzymatic gating of voltage-gated Ca channels. *Ann. NY Acad. Sci.* 635: 26–34.

Arreola, J., R. T. Dirksen, R.-C. Shieh, D. J. Williford, and S.-S. Sheu. 1991. Ca current and current transients under action potential clamp in guinea-pig ventricle myocytes. *Am. J. Physiol.* 261:C393–C397.

Ashcroft, F. M., and P. R. Standfield. 1981. Ca-dependence of the inactivation of Ca currents in skeletal muscle in insect. *Science (Wash. DC).* 213:224–226.

Bean, B. P. 1985. Two kinds of Ca channels in canine atrial cells. *J. Gen. Physiol.* 86:1–30.

Bean, B. P. 1989. Multiple types of Ca channels in heart muscle and neurons. *Ann. NY Acad. Sci.* 560:334–345.

Brehm, P., and R. Eckert. 1978. Ca entry leads to inactivation of Ca current in *Paramecium*. *Science (Wash. DC).* 202:1203–1206.

Brehm, P., R. Eckert, and D. Tillotson. 1980. Ca-mediated inactivation of Ca current in *Paramecium*. *J. Physiol. (Lond.).* 306:193–203.

Cannell, M. B., J. R. Berlin, and W. J. Lederer. 1987. Effect of membrane potential changes on the Ca transient in single rat cardiac muscle cells. *Science (Wash. DC).* 238:1419–1423.

Catterall, W. 1991. Functional subunit structure of voltage-gated Ca channels. *Science (Wash. DC).* 253:1551–1553.

Cavalie, A., R. Ochi, D. Pelzer, and W. Trautwein. 1983. Elementary currents through Ca channels in guinea-pig myocytes. *Pfluegers Arch. Eur. J. Physiol.* 398:284–297.

Cavalie, A., D. Pelzer, and W. Trautwein. 1986. Fast and slow gating behavior of single Ca channels in cardiac cells. Relation to activation and inactivation of Ca-channel current. *Pfluegers Arch. Eur. J. Physiol.* 406: 241–258.

Chad, J. E., and R. Eckert. 1984. Ca domains associated with individual Ca currents can account for anomalous voltage relations of Ca-dependent responses. *Biophys. J.* 45:993–999.

Cleemann, L., and M. Morad. 1991. Role of Ca channel in cardiac excitation-contraction coupling in the rat: evidence from Ca transients and contraction. *J. Physiol. (Lond.).* 432:283–312.

DeFelice, L. J. 1993. Molecular biology and biophysics of Ca channels. *J. Membr. Biol.* 133:191–202.

DeFelice, L. J., W. Goolsby, and M. Mazzanti. 1989. K channels and the repolarization of cardiac cells. *In* Embryonic Origins of Defective Heart Development. M. Kirby, and D. Bockman, editors. *Ann. N. Y. Acad. Sci.* 558:174–184.

DeFelice, L. J., Y.-M. Liu, S. Risso, and M. Mazzanti. 1991. Ca channel kinetics during the spontaneous heart beat in embryonic chick ventricle. *Biophys. J.* 59:551*a*. (Abstr.)

Doerr, T., R. Denger, and W. Trautwein. 1989. Ca currents in single SA nodal cells of the rabbit heart studied with action potential clamp. *Pfluegers Arch. Eur. J. Physiol.* 413:599–603.

Doerr, T., R. Denger, and W. Trautwein. 1990. Ionic currents contributing to the action potential in single ventricular myocytes of the guinea-pig studied with action potential clamp. *Pfluegers Arch. Eur. J. Physiol.* 416: 230–237.

Fujii S., R. K. Ayer, and R. L. DeHaan. 1988. Development of the fast Na current in early embryonic chick heart cells. *J. Membr. Biol.* 101:209–223.

Hadley, R. W., and J. R. Hume. 1987. An intrinsic potential-dependent inactivation mechanism associated with Ca channels in guinea-pig myocytes. *J. Physiol. (Lond.).* 389:205–222.

Hadley, R. W., and W. J. Lederer. 1991. Ca and voltage inactivate Ca channels in guinea-pig ventricular myocytes through independent mechanisms. *J. Physiol. (Lond.).* 44:257–268.

Hagiwara, S., and S. Najaima. 1966. Effects of intracellular Ca concentrations upon the excitable of the muscle fiber membrane of a barnacle. *J. Gen. Physiol.* 49:870–818.

Hartzell, H. C. 1988. Regulation of cardiac ion channels by catecholamines, acetylcholine and second messenger systems. *Prog. Biophys. Mol. Biol.* 52:165–247.

Hartzell, H. C., P.-F. Mèry, R. Fischmeister, and G. Szabo. 1991. Sympathetic regulation of cardiac Ca current is due exclusively to cAMP-dependent phosphorylation. *Nature (Lond.).* 351:573–576.

Hess, P., and R. W. Tsien. 1984. Mechanism of ion permeation through Ca channels. *Nature (Lond.).* 309:453–456.

Hess, P., J. B. Lansman, and R. W. Tsien. 1984. Different modes of Ca channel gating behavior favoured by dihydropyridine Ca agonists and antagonists. *Nature (Lond.).* 311:538–544.

Hess, P., J. B. Lansman, and R. W. Tsien. 1986. Ca channel selectivity for divalent and monovalent cations. *J. Gen. Physiol.* 88:293–319.

Hirano, Y., C. T. January, and H. A. Fozzard. 1989. Characteristics of L and T Ca currents in canine cardiac Purkinje cells. *Am. J. Physiol.* 256: H1478–H1492.

Hodgkin, A. L., and A. F. Huxley. 1952. A qualitative description of membrane current and its application to conduction in nerve. *J. Physiol. (Lond.).* 117:440–544.

Imredy, J. P., and D. T. Yue. 1992. Submicroscopic Ca diffusion mediates inhibitory coupling between individual Ca channels. *Neuron.* 9:197–207.

Josephson, I., and N. Sperelakis 1990. Fast activation of cardiac Ca channel gating charge by the dihydropyridine agonist, BAY K 8644. *Biophys. J.* 58:1307–1311.

Kass, R. S., and M. C. Sanguinetti. 1984. Inactivation of Ca channel current in the calf cardiac Purkinje fiber. Evidence for the voltage- and Ca-mediated mechanisms. *J. Gen. Physiol.* 84:705–726.

Kawano, S., and R. L. DeHaan. 1989. Low threshold current is major Ca current in embryonic chick ventricle cells. *Am. J. Physiol.* 256: H1505–1508.

Klockner, U., and G. Isenberg. 1991. Currents through single L-type Ca channels studied at 2 mM $[Ca]_o$ and 36°C in myocytes from urinary bladder of the guinae-pig. *J. Physiol. (Lond.).* 438:228P.

Klockner, U., A. Scheifer, and G. Isenberg. 1990. L-type Ca channels: similar Q10 of Ca-, Ba-, and Na-conductance points to the importance of ion-channel interactions. *Pfluegers Arch. Eur. J. Physiol.* 415:638–641.

Kokubun, S., and H. Reuter. 1984. Dihydropyridine derivatives prolong the open state of Ca channels in cultured cardiac cells. *Proc. Natl. Acad. Sci. USA.* 81:4824–4827.

Lacerda, A. E., and A. M. Brown. 1989. Nonmodal gating of cardiac Ca channels as revealed by dihydropyridines. *J. Gen. Physiol.* 93:1243–1273.

Lansman, J. B., P. Hess, and R. W. Tsien. 1986. Blockade of current through single Ca channels by Cd, Mg, and Ca. *J. Gen. Physiol.* 88:321–347.

Lederer, W. J., E. Niggli, and R. W. Hadley. 1990. Na-Ca exchange in excitable cells: fuzzy space. *Science (Wash. DC).* 248:283.

Lee, K. S., E. Marban, and R. W. Tsien. 1985. Inactivation of Ca channels in mammalian heart cells: joint dependence on membrane potential and intercellular Ca. *J. Physiol. (Lond.).* 364:395–411.

Levi, R., and L. J. DeFelice. 1986. Na-conducting channels in cardiac membranes in low Ca. *Biophys. J.* 50:5–9.

Lew, W., L. W. Hryshko, and O. M. Bers. 1991. DHP receptors are primarily functional L-type Ca channels in rabbit ventricular myocytes. *Circ. Res.* 69:1139–1145.

Llinas, R., M. Sugimori, and R. B. Silver. 1992. Microdomains of high Ca concentration in a presynaptic terminal. *Science (Wash. DC).* 256:677–679.

Lux, H. D., and A. M. Brown. 1984. Single channel analysis on inactivation of Ca channels. *Science (Wash. DC).* 225:432–434.

Mazzanti, M., and L. J. DeFelice. 1987a. Regulation of the Na-conducting channel during the cardiac action potential. *Biophys. J.* 51:115–121.

Mazzanti, M., and L. J. DeFelice. 1987b. Na channel kinetics during the spontaneous heart beat in embryonic chick ventricle cells. *Biophys. J.* 52:95–100.

Mazzanti, M., and L. J. DeFelice. 1988. K channel kinetics during the spontaneous heart beat in embryonic chick ventricle cells. *Biophys. J.* 54: 1139–1148.

Mazzanti, M., and L. J. DeFelice. 1990. Ca channel gating during cardiac action potentials. *Biophys. J.* 58:1059–1065.

Mazzanti, M., L. J. DeFelice, and Y.-M. Liu. 1991. Gating of L-type Ca channels in embryonic chick ventricle cells: dependence on voltage, current and channel density. *J. Physiol. (Lond.).* 443:307–334.

McDonald, T. F., A. Cavalie, W. Trautwein, and D. Pelzer. 1986. Voltage-dependent properties of macroscopic and elementary Ca channel currents in guinea-pig ventricular myocytes. *Pfluegers Arch. Eur. J. Physiol.* 406: 437–448.

Mentrard, D., G. Vassort, and R. Fischmeister. 1984. Ca-mediated inactivation of the Ca conductance in Cs-loaded frog heart cells. *J. Gen. Physiol.* 83:105–131.

Mikami, A., K. Imoto, T. Tanabe, T. Niidome, Y. Mori, H. Takeshima, S. Narumiya, and S. Numa. 1989. Primary structure and functional expression of the cardiac dihydropyridine-sensitive Ca channel. *Nature (Lond.).* 340:230–233.

Mori, Y., T. Friedrich, Kim Man-Suk, et al. 1991. Primary structure and functional expression from cDNA of a brain Ca channel. *Nature (Lond.).* 350:398–402.

Nargeot, J., N. Dascal, and H. A. Lester. 1992. Heterologous expression of Ca channels. *J. Membr. Biol.* 126:97–108.

Nilius, B., P. Hess, B. Lansman, and R. W. Tsien. 1985. A novel type of cardiac Ca channel in ventricular cells. *Nature (Lond.).* 316:443–446.

Nowycky, M. C., A. Fox, and R. W. Tsien. 1985. Long-opening mode of gating of neuronal Ca channels and its promotion by the dihydropyridine Ca agonist Bay K 8644. *Proc. Natl. Acad. Sci. USA.* 82:2178–2182.

Ochi, R., and Y. Kawashima. 1990. Modulation of slow gating process of Ca channels by isoprenaline in guinea-pig ventricular cells. *J. Physiol. (Lond.).* 424:157–204.

Osaka, T., and R. W. Joyner. 1991. Developmental changes in Ca channels of rabbit ventricular cells. *Cir. Res.* 68:788–796.

Perez-Reyes, E., A. Castellano, H. S. Kim, P. Bertrand, E. Baggstrom, A. E. Lacerda, X. Wei, and L. Birnbaumer. 1992. Cloning and expression of a cardiac/brain β subunit of the L-type Ca channel. *J. Biol. Chem.* 267: 1–6.

Reuter, H., C. F. Stevens, R. W. Tsien, and G. Yellen. 1983. Properties of single Ca channels in cardiac cell culture. *Nature (Lond.).* 297:501–504.

Roberts, W. M., R. A. Jackobs, and A. J. Hudspeth. 1990. Colocalization of ion channels involved in frequency selectivity and synaptic transmission at presynaptic active zones of hair cells. *J. Neurosci.* 10:3664–3684.

Risso S., L. J. DeFelice, and W. N. Goolsby. 1992. A mathematical model that incorporates channel density and describes the kinetics of Ca channels in nerve and heart during the action potential. *Biophys. J.* 61:248*a*. (Abstr.)

Singer, D., M. Biel, I. Lotan, V. Flockerzi, F. Hofmann, and N. Dascal. 1991. The roles of the subunits in the function of the Ca channels. *Science (Wash. DC).* 253:1553–1556.

Sigworth, F. J., and E. Neher. 1980. Single Na channel currents observed in cultured rat muscle cells. *Nature (Lond.).* 287:447–449.

Soong, T. W., T. Soong, A. Stea, C. Hodson, S. Dubel, S. Vincent, and T. Snutch. 1993. Structure and functional expression of a member of the low voltage-activated CA channel family. *Science (Wash. DC).* 260:1133–1136.

Standen, N. B., and P. R. Stanfield. 1982. A binding-site model for Ca channel inactivation that depends on Ca entry. *Proc. R. Soc. Lond. B Biol. Sci.* B217:101–110.

Tillotson, D. 1979. Inactivation of Ca conductance dependent upon entry of Ca ions in Molluscan neurons. *Proc. Natl. Acad. Sci. USA.* 76:1479–1500.

Trautwein, W. 1984. Beta-adrenergic increase in the Ca conductance of cardiac myocytes studied with the patch clamp. *Pfluegers Arch. Eur. J. Physiol.* 401:111–118.

Tsien, R. W., P. T. Ellinor, and W. A. Horne. 1991. Molecular diversity of voltage-dependent Ca channels. *Trends Pharmacol. Sci.* 12:349–354.

Tytgat, J., B. Nilius, J. Vereecke, and E. Carmeliet. 1988. The T-type Ca channel in guinea-pig ventricular myocytes is insensitive to isoproterenol. *Pfluegers Arch. Eur. J. Physiol.* 411:704–706.

Varadi, G., P. Lory, D. Schultz, M. Varadi, and A. Schwartz. 1991. Acceleration of activation and inactivation by the β subunit of the skeletal muscle Ca channel. *Nature (Lond.).* 352:159–162.

Wellis, D., L. J. DeFelice, and M. Mazzanti. 1990. Outward Na current in beating heart cells. *Biophys. J.* 57:41–48.

Williams, M. E., P. F. Brust, D. H. Feldmann, et al. 1992. Structure and functional expression of an x-conotoxin-sensitive human N-type Ca channel. *Science (Wash. DC).* 257:389–395.

Yue, D. T., and E. Marban. 1990. Permeation in the dihydropyridine-sensitive Ca channel: multi-ion occupancy but no mole fraction effect between Ba and Ca. *J. Gen. Physiol.* 95:911–939.

Yue, D. T., S. Herzig, and E. Marban. 1990. β-Adrenergic stimulation of Ca channels occurs by potentiation of high-activity gating modes. *Proc. Natl. Acad. Sci. USA.* 87:753–757.

Yue, D. T., P. H. Backx, and J. P. Imredy. 1991. Ca-sensitive inactivation in the gating of single Ca channels. *Science (Wash. DC).* 250:1735–1738.